

Electronic Supplementary Information (ESI) for: Ultrafast excited-state dynamics of isocytosine

Rafał Szabla,^{*a} Robert W. Góra,^{*b} and Jiří Šponer^{a,c}

June 1, 2016

Table 1 Spin-orbit coupling matrix elements [cm^{-1}] calculated for the S_1 minimum energy geometries of *keto*-iC and *enol*-iC. The sum of squares of SOC matrix elements (given in cm^{-2}) is denoted as $|\mathcal{H}_{SO,i}|^2$.

Component	$S_1 \rightsquigarrow T_1$	$S_1 \rightsquigarrow T_2$
<i>enol</i> -iC		
$\mathcal{H}_{SO,x}$	0	0
$\mathcal{H}_{SO,y}$	2.184	4.198
$\mathcal{H}_{SO,z}$	0	0
$ \mathcal{H}_{SO,i} ^2$	4.8	17.6
<i>keto</i> -iC		
$\mathcal{H}_{SO,x}$	32.368	2.681
$\mathcal{H}_{SO,y}$	37.982	3.021
$\mathcal{H}_{SO,z}$	32.368	2.681
$ \mathcal{H}_{SO,i} ^2$	3538.0	23.5

Table 2 Relative energies (in eV) of the most important MECPs calculated with respect to the energy of the ground electronic state at the equilibrium geometry. The MECPs were optimized using the ADC(2)/MP2 method. The additional value provided in parenthesis for the $n\pi^*/S_0$ MECP of *keto*-iC was calculated for the conical intersection optimized using the MR-CISD/SA-2-CASSCF(6,5)/cc-pVDZ method since the corresponding geometry obtained at the ADC(2)/MP2 level was unreliable.

MECP type	ADC(2)/MP2/aug-cc-pVDZ	NEVPT2/SA-CASSCF(8,7)/cc-pVTZ
<i>enol</i> -iC		
$\pi\pi^*/S_0$ (ring-puckering)	4.30	5.05
$\pi\pi^*/S_0$ (C=C twisting)	4.17	4.55
<i>keto</i> -iC		
$n\pi^*/S_0$ (N-H tilting/C=O stretching)	3.65	5.54 (6.10)
$\pi\pi^*/S_0$ (ring-puckering)	3.63	4.37

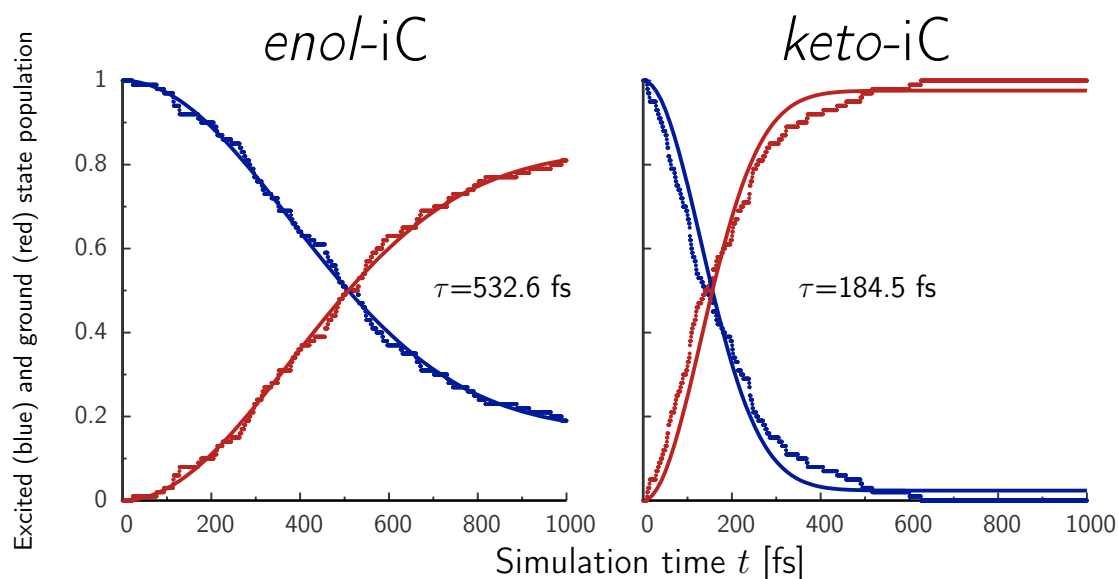


Fig. 1 Excited-state lifetimes and population fittings obtained using the sigmoid function: $f(t) = f_0 + (1 - f_0) \exp\left[-\left(\frac{t}{\tau}\right)^2\right]$. Blue (red) dots indicate excited (ground) state populations, while solid lines show the fitted curves.

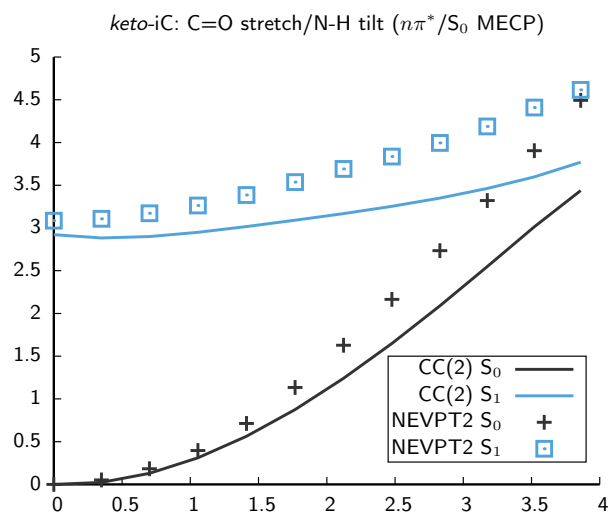


Fig. 2 Linear interpolation in internal coordinates between the S_1 minimum of *keto-iC* and the $n\pi^*/S_0$ conical intersection optimized using the MRCISD(6,5) method. The lines present PE curves for the CC2/aug-cc-pVDZ method, while the points show the reference values obtained at the NEVPT2/SA-CASSCF(8,7)/cc-pVTZ level (see also Fig. 9 in the main article for the corresponding ADC(2) values). Even though the CC2 energies predict slightly more sloped topology of this MECP, the CC2 PE surfaces disagree with the reference NEVPT2 values. This suggests that the highly multireference character of the ground-state wave function at the $n\pi^*/S_0$ MECP cannot be correctly reproduced neither by the ADC(2)/MP2 nor by CC2 methods.

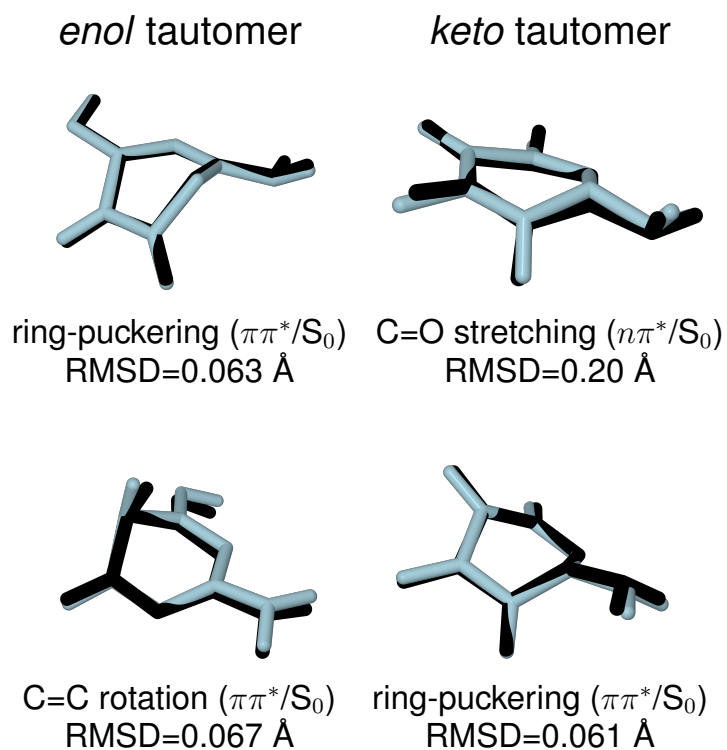


Fig. 3 Comparison of the geometries of conical-intersections optimized at the MR-CISD/SA-2-CASSCF(2,2)/cc-pVDZ level (black) and MECs obtained at the ADC(2)/MP2 level (light blue). The smallest reference space in the MR-CISD calculations partly reproduced the multireference character of the $n\pi^*/S_0$ MEC and suggested the inaccuracy of the ADC(2)/MP2 methods at this state crossing. Since a larger reference space was necessary to correctly reproduce the features of the $n\pi^*/S_0$, we focused on the calculations at the MR-CISD/SA-2-CASSCF(6,5)/cc-pVDZ level in the main article.